# “Afterlife Experiment”: use of MALDI-MS and SIMS imaging for the Study of the nitrogen cycle within plants

SEAMAN, Callie, FLINDERS, Bryn, EIJKEL, Gert, HEEREN, Ron M.A., BRICKLEBANK, Neil <http://orcid.org/0000-0002-1614-2260> and CLENCH, Malcolm R. <http://orcid.org/0000-0002-0798-831X>



**Published version**

SEAMAN, Callie, FLINDERS, Bryn, EIJKEL, Gert, HEEREN, Ron M.A., BRICKLEBANK, Neil and CLENCH, Malcolm R. (2014). “Afterlife Experiment”: use of MALDI-MS and SIMS imaging for the Study of the nitrogen cycle within plants. Analytical Chemistry, 86 (20), 10071-10077.

# The "Afterlife Experiment" : Use of MALDI-MS and SIMS Imaging for the Study of the Nitrogen Cycle within Plants

Callie Seaman[1], Bryn Flinders[2], Gert Eijkel[2], Ron M.A. Heeren[2], Neil Bricklebank[1] and Malcolm R Clench[1]

[1.] Biomedical Research Centre, City Campus, Sheffield Hallam University, Howard Street, Sheffield, S1 1WB

[2.] FOM Institute AMOLF, Science Park 104, 1098 XG Amsterdam, The Netherlands

Callie Seaman callie.a.seaman@student.shu.ac.uk, Bryn Flinders b.flinders@amolf.nl, Gert Eijkel g.eijkel@amolf.nl, Ron M.A. Heeren r.heeren@amolf.nl, Neil Bricklebank n.bricklebank@shu.ac.uk, Malcolm R Clench m.r.clench@shu.ac.uk.

Title Running Head: The "Afterlife Experiment" : Use of MALDI-MS and SIMS Imaging for the Study of the Nitrogen Cycle within Plants

Corresponding author*: Prof. Malcolm Clench, tel +441142253054, fax +441142253064, email: m.r.clench@shu.ac.uk

**Abstract**

As part of a project to demonstrate the science of decay a series of mass spectrometry imaging experiment were performed. The aim was to demonstrate that decay and decomposition are only a part of the story and to show pictorially that atoms and molecules from dead plants and animals are incorporated into new life. "Caliente" leaf mustard plants (84% Brassica juncea, 16% *Sinapsis Alba*) were grown hydroponically using a nutrient system containing $^{15}N$ $KNO_3$ (98% labelled) as the only source of nitrogen. Plants were cropped and left to ferment in water for two weeks to create a mustard "tea". The mustard "tea" was used a source of nitrogen for a second hydroponics experiment where radish (*Raphanus sativus*) plants were grown in an experiment set up in a sealed container within the chimpanzee house of Edinburgh Zoo. After five weeks of growth radish were harvested sent to Sheffield where they were cryosectioned and sections imaged by positive ion MALDI imaging and LDI imaging mass spectrometry. The presence of labelled $NO_3^-$ in the both plants grown using $^{15}N$ $KNO_3$ as nutrient and those grown from the mustard "tea" was readily discernable. Subsequent to the programme uptake of $^{15}N$ into a number of identifiable metabolites has been studied by MALDI-MS imaging and SIMS imaging.

**Keywords:** MALDI-MSI, MetA-SIMS, $^{15}N$, choline.

## 1.0. Introduction

In May 2011 the MS Imaging group at Sheffield Hallam University was approached by the BBC to take part in a project to demonstrate the science of decay[1]. Set up in Edinburgh Zoo in summer 2011 a fully equipped kitchen and garden together with all the detritus from a family barbeque was sealed in a glass box. The programme a joint venture between the BBC and the Discovery Channel followed the events as maggots, moulds, bacteria, flies and mushrooms transformed the contents beyond all recognition. As part of the experiment the programme makers wished to demonstrate that decay and decomposition was only part of the story with atoms and molecules from dead plants and animals being incorporated into new life.

The element nitrogen is a ubiquitous component of all living systems and is located, primarily, in amino acids, proteins, nucleic acids and, in plants, chlorophyll. Nitrogen is one of the principal nutritional requirements of all plants which acquire it through their root systems, usually in the form of nitrates. In the plant the nitrate is quickly converted into nitrites and then ammonium ions which can be assimilated into amino acids[2]. The nitrogen cycle has been extensively documented, research into the nitrogen cycle first started in 19$^{th}$ century, with scientist such as Boussingault shaping modern agrochemistry[3].

There have been many studies of the uptake and metabolization of nitrogen by plants and many of these utilise the isotope $^{15}N$; this is a rare but stable isotope, with a natural abundance of 0.366% (0.00366 mole fractions)[4,5]. Plant studies utilizing $^{15}N$ enriched $KNO_3$ material as a tracer in isotopic analysis are well documented, with techniques such as gas chromatography–mass spectrometry (GC-MS)[6], inductively coupled plasma-optical emission spectroscopy (ICP-OES)[7], microwave induced plasma-optical emission spectroscopy (MIP-OES)[8], nuclear magnetic resonance (NMR)[9], , liquid chromatography-tandem mass spectrometry (LC-MS/MS)[6], multi-isotope imaging mass spectrometry (MIMS)[10] and secondary ion mass spectrometry (SIMS)[11] all being employed. Furthermore, it has been used in agricultural research to trace mineral nitrogen compounds (particularly fertilizers) in the environment and is also a very important tracer for describing the fate of nitrogenous organic pollutants[12,13].

Matrix-assisted laser/desorption ionisiontion-mass spectrometry imaging (MALDI-MSI) is an emerging technique within plant biology[14]. In the past MALDI-MSI has been used to illustrate the distribution of various plant metabolites[15-17], including carbohydrates[18], oligosaccharides[19], proteins[20,21], lipids[22,23], peptides[24], pesticides[25] and various agrochemicals[26] within plant tissue. Until now the use of this technique to study nutrient cycles within plants has not been described. The work reported here aimed to demonstrate that mass spectrometry imaging is a valuable tool in the tracking of the distribution of $^{15}N$ labeled $NO_3^-$ and can be used to show uptake of species from dead organisms by living ones.

## 2.0. Experimental

### 2.1. Materials

Alpha-cyano-4-hydroxycinnamic acid (CHCA), Choline chloride, 99%, 4-Aminobutyric acid, 99+%, Methanol, acetonitrile, Trifluoroacetic acid (TFA) (AR Grade), were purchased from Fisher Scientific (Loughborough, UK). Calcium chloride, Calcium sulphate, magnesium sulphate, potassium phosphate and a trace element mix were all purchased from Hortifeeds (Lincoln, UK). 2, 5-dihydroxybenzoic acid (DHB), Potassium nitrate-$^{15}N$ 98 atom % $^{15}N$ ($^{15}N$- $KNO_3$), Potassium nitrate *ReagentPlus*®, ≥99.0% were purchased from Sigma-Aldrich (Gillingham, UK).

2.2. Cultivation (Hydroponic Experiment)

Two groups of radish seeds (*Raphanus sativus*) were sown in a mix of perlite and vermiculite (4:3) in an artificially controlled environment.

The control group utilized a nutrient system containing standard $KNO_3$, the second group ($^{15}N$) replaced all of the $KNO_3$ with $^{15}N$ $KNO_3$ (98% labelled) as the only source of nitrogen. Plants were cropped, homogenised and left to ferment in water for two weeks to create a "tea". The "tea" was used a source of nitrogen for a second hydroponics experiment (Second generation) where radish (*Raphanus sativus*) were grown in an artificially controlled environment. After five weeks of growth radish plants were harvested. Samples of leaves, bulbs, and stems from each group (Control, $^{15}N$ and Second Generation) were cryosectioned and sections imaged by positive ion MALDI imaging. (Figure 1)

2.3. Sample Preparation

The radishes were harvested and the bulbs separated from the roots and leaves and snap frozen in liquid nitrogen. The frozen radish bulbs were sectioned at a temperature of -20°C using a Leica Cryostat (Leica, Wetzlar, Germany) to obtain 12 µm sections, which were thaw mounted onto glass slides and ITO slides. Leaves were prepared by placing fresh samples between tissue paper and pressing between two glass slides. The slides were tapped together and placed into a freeze drier at -36°C until they reached a constant mass, approximately ten days. The dried leaves were mounted onto either aluminium target plates or glass slides using carbon tape to adherer the sample.

2.3.1. MALDI Matrix Deposition

Samples for MALDI were coated with a 5mg/ml solution of CHCA in 70:30 methanol: water with 0.2% TFA using the Suncollect™ automated pneumatic sprayer (Sunchrom GmbH, Friedrichsdorf, Germany) in a series of 10 layers. The initial seeding layer was performed at 2µl/minute and subsequent layers were performed at 3µl/minute. Samples were also coated with a 20 mg/ml solution of DHB in 50:50 acetonitrile: water with 0.2% TFA using the Suncollect™ automated pneumatic sprayer in a series of 30 layers. The initial seeding

105 layer was performed at 10µl/minute then stepped up to 20 µl/minute and subsequent layers were performed at
106 30µl/minute.
107
108 2.3.2. SIMS Sample Gold Coating
109 Prior to analysis the radish tissue sections were gold-coating using a Quorum Technologies SC7640 sputter
110 coater (New Haven, USA) equipped with a FT7607 quartz crystal microbalance stage and FT690 film
111 thickness monitor to deposit a 1 nm thick gold layer
112
113 2.4. Instrumentation
114 2.4.1. Applied Biosystems Q-Star Pulsar I
115 Initial mass spectrometric analyses were performed using a Applied Biosystems API Q-Star Pulsar i hybrid
116 quadrupole time-of-flight (QTOF) instrument (Concord, Ontario, Canada) fitted with an orthogonal MALDI
117 ion source and a 1 kHz Nd:YAG solid-state laser. Images were acquired at a spatial resolution of 150µm x
118 150µm in "raster image" mode[27], using 'oMALDI Server 5.1' software supplied by MDS Sciex (Concord,
119 Ontario, Canada) and generated using the freely available Biomap 3.7.5.5 software (Novartis, Basel,
120 Switzerland). Mass spectra were processed either in Analyst MDS Sciex (Concord,Ontario,Canada) or using
121 the open source multifunctional mass spectrometry software mMass[28].
122
123 MALDI MS spectra were obtained in positive ion mode in the mass range between *m/z* 50 and 1000.
124 Declustering potential 2 was set at 15 arbitrary units and the focus potential at 10 arbitrary units, with an
125 accumulation time of 0.999 sec. Average spectra were acquired over a 0.5 $cm^2$ region on the leaves. The
126 MALDI MS/MS spectrum of the unknown precursor ions at m/z 104.1 and 105.1 was obtained using argon as
127 the collision gas; the declustering potential 2 was set at 15 and the focusing potential at 20, and the collision
128 energy and the collision gas pressure were set at 20 and 5 arbitrary units, respectively.
129
130 2.4.2. Waters Synapt G2 HDMS
131 Further MALDI data were acquired using a Waters MALDI SYNAPT™ G2 HDMS mass spectrometer
132 (Waters Corporation, Manchester, UK) to acquire mass spectra and images. Prior to MALDI-MSI analysis the
133 samples were optically scanned using a flatbed scanner to produce a digital image for future reference, this
134 image was then imported into the MALDI imaging pattern creator software (Waters Corporation) to define the
135 region to be imaged. The instrument was calibrated prior to analysis using a standard mixture of polyethylene
136 glycol. The instrument was operated in V-mode and positive ion mode, all data was acquired in the mass
137 range m/z 100 to 500. The data was then converted using MALDI imaging converter software (Waters
138 Corporation) and visualised using the BioMap 3.7.5.5 software (Novartis, Basel, Switzerland).
139 2.4.3. MetA-SIMS imaging

SIMS data was acquired using a Physical Electronics TRIFT II TOF-SIMS (Physcial Electronics, USA) equipped with an Au liquid metal gun tuned for 22keV Au+ primary ions. Images were acquired in mosaic mode using 64 tiles that each measures 125 μm square and contains 256x256 pixels. The total area scanned was 1 x 1 mm area with 60 seconds/tile resulting in a total of 4194304 spectra.

2.5 Data processing

Images from the Q-Star instrument were processed using Biomap 3.7.5.5 software. All images were normalised against the total ion count (TIC). For presentation purposes, the mass spectra from the Analyst QS 1.1 software was exported in the form of a text file and then imported into the mMass software for processing. MALDI-MSI data from the Waters Synapt instrument was converted into Analyze 7.5 format using MALDI imaging converter software (Waters Corporation) and visualised using the BioMap 3.7.5.5 software (Novartis, Basel, Switzerland).

SIMS data were analysed and visualized using WinCadence software version 4.4.0.17 (Physical Electronics).

**Results and Discussion**

Previous work has demonstrated that plants quickly metabolise nitrogen in to amino acids after assimilation via the roots[2]. Initially glutamine and glutamate were investigated, as these are the primary amino acids formed from nitrogen uptake. Other amino acids were also investigated with particular attention to arginine (m/z 175) as previous work using MALDI-MSI had demonstrated its distribution within plants[16]. The focus on these particular amino acids was intended to demonstrate the incorporation of nitrogen from the now dead radish plants into protein synthesis for the new living plants, however unambiguous identification of these amino acids proved difficult owing to the complex overlapping isotope peaks present in this region of the positive ion mass spectrum.

However the B-complex vitamin Choline, ($C_5H_{14}NO$), *m/z* 104.1, was found to have incorporated the labelled $^{15}N$, producing an ion with *m/z* 105.1. These data are presented as Figure 2 and 3. Further identification of these peaks as arising from Choline is supported by the MALDI MS/MS data presented in Figure S1. Figure S1 confirms the identification of the *m/z* 104 and *m/z* 105 ions as choline and $^{15}N$ labelled choline respectively, clearly showing the appropriate product ions. The spectrum produced matched that generated data by the Scripps Centre for Metabolomics. The product ions from of the $^{15}N$ radish bulb and leaves have all increased in mass to charge by one, Figure S1b, which further confirms the identification.

The main distribution of the choline within the bulbs was found to be near to the skin, but not actually within the skin. It was also widely distributed though the bulb (Figure 2). This is supported by the distribution of pelargonidin ($[M+H]^+$ m/z 271). This is a natural food colouring found in radish skin, when overlaid with the Choline, it can be clearly seen that these species exist in two distinct and separate areas. (Data not show)

The MALDI-MS images in figure 2 show the full extent of distribution of the labelled and the unlabelled choline. The MALDI-MS spectra of the three leaves in figure 3, also reveals the difference in the intensity of the labelled (*m/z* 105) and unlabelled (*m/z* 104) choline. Figure 3a shows a higher intensity of the unlabelled choline (*m/z* 104), whereas 3b shows a higher intensity of labelled Choline (*m/z* 105), confirming that the $^{15}N$ was metabolised by the plant and incorporated in to its structure. Figure 3c demonstrates that the $^{15}N$ was then passed from the first generation to the second generation radish that was grown with plant material that had been feed exclusively $^{15}N$ nitrogen. The even intensity and distribution of labelled and unlabelled choline can be clearly seen in figures 2 and 3c.

The MALDI-MS spectrum (Figure 3c) shows that approximately 50% of the material from the first generation radishes has successfully been transferred and assimilated into the formation of the second generation radish. This is also visually reflected in the MALDI-MS images shown in Figures 2 and 4, which shows the same distribution with equal intensity for the labelled and un-labelled choline and phosphocholine.

The MALDI-MS images displayed in Figure 4 show the distribution of labelled and un-labelled species in the second generation radish section, following normalization against the total ion current (TIC). The species at m/z 271 (Figure 4a) appears to be exclusively localized within the skin of the radish tissue section. This has been tentatively identified as the anthrocyanidin pelargonidin which is the natural food colour in the radish skin[29]. In order to confirm this assignment MS/MS was performed and the resulting spectrum Figure S2 matched that of the reference MS/MS data independently generated by the Scripps Center for Metabolomics. The distributions of the un-labelled and labelled choline at m/z 104 and 105 (Figures 4b and 4c respectively) are predominantly in the centre of the radish tissue. This is also observed with un-labelled and labelled phosphocholine at m/z 184 and 185 (Figures 4d and 4e respectively). The distributions of labelled choline and phosphocholine at m/z 105 and 185 were overlaid with the distribution of pelargonidin at m/z 271, which is shown in Figures 4f and 4g. These images demonstrate that there is a clear distinction between the two regions and that the labelled species are only present in the centre of the radish.

The metal assisted-secondary ion mass spectrometry (MetA-SIMS) images of the control radish are displayed in Figure 5. The optical image (Figure 5a) shows a magnified view of the centre portion of the radish, which looks like that of the first generation radish. The TIC image is shown in Figure 5b. The MetA-SIMS images of the control radish show the distribution of un-labelled choline at m/z 104 (Figure 5c) and the isotope of this peak at m/z 105 (Figure 5d). The mass spectrum (Figure 5e) shows a strong peak at m/z 104 which has been

tentatively assigned to the un-labelled choline. This is expected to be the abundant form as this radish was grown exclusively with an un-labelled compound.
The isotopic ratio (m/z 104/ m/z 105) for the control radish is 2.5322.

The MetA-SIMS images displayed in Figure 6 shows the distribution of labelled and un-labeled choline in the first generation radish section. The optical image (Figure 6a) shows a magnified view of the centre portion of the radish, the TIC image is shown in Figure 6b. The MetA-SIMS images of un-labelled choline at m/z 104 and $^{15}N$ labelled choline at m/z 105 (Figures 6c and 6d respectively) show both species are widely distributed in the string like network observed in the optical image. The related spectrum (Figure 6e) shows a strong peak at m/z 105 which could be $^{15}N$ labelled choline, which is expected as this radish was grown exclusively with a $^{15}N$ labelled compound. The isotopic ratio for the first generation radish was calculated from the SIMS data to be 0.1963.

The MetA-SIMS images of the second generation radish displayed in Figure 7 shows the distribution of labelled and un-labelled choline. The optical image (Figure 7a) shows a magnified view of the centre portion of the radish, which looks more homogenous than the first generation radish. The TIC image is shown in Figure 7b. The MetA-SIMS images of un-labelled choline at m/z 104 (Figure 7d) and $^{15}N$ labelled choline at m/z 105 (Figures 7c) show both species are evenly distributed through the imaged area. The related spectrum (Figure 7e) again shows a peak at m/z 105 which could be $^{15}N$ labelled choline, however neither the images nor the spectrum reflect the same pattern previously observed in the MALDI-MS data of the second generation radish. The isotopic ratio calculated for the second generation radish is 0.4689. This variation could be due to the presence of an unidentified peak at *m/z* 105, which is often observed during TOF-SIMS analysis of gold coated samples. The labelled choline at *m/z* 105 is shadowed due to this strong ion presence. This peak was also observed in the spectrum from the control radish, in this spectrum the peak appears to be half the intensity of the un-labelled choline at *m/z* 104 and therefore is not an isotope.

Whilst previous studies using isotopes such as $^{14}C$, $^{15}N$ and $^{31}P$ have demonstrated the cycle of these key nutrients for plant[5-8,12,13], the techniques used *i.e.* s inductively coupled plasma-mass spectrometry (ICP-MS)[10,30], GC-MS[6], ICP-OES[7], MIP-OES[8], NMR[9] and LC-MS/MS[6] were employed to show a general distribution of the nitrogen within the tissue, as all of these methods require the tissue to be destroyed either by a digestion or extraction method prior to analysis. Imaging techniques have been used to study plants extensively including laser ablation-inductively coupled plasma-mass spectrometry (LA-ICP-MS)[15,31-33], X-ray absorption spectroscopy (XAS)[31,33], X-ray fluorescence (XRF)[31,33], SIMS[10,15,31,33] and MALDI-MS[14-

[17,20,22,23] but the data presented here is the first use of mass spectrometry imaging to demonstrate unambiguously that atoms and molecules move from dead plant material into new living material.

This is also the first demonstration of the use of MALDI-MS and SIMS imaging to show the distribution, translocation and metabolism of nitrogen in plants. MALDI-MS imaging of plant material is a relatively new technique, with only a small number of researchers performing it. Compounds such as nicosulfuron[25] and other agrochemicals compounds[26] have previously been monitored using this technique, but no demonstration of the cycle of this compound was performed. Other naturally occurring compounds in plants to be monitored and mapped using MALDI-MS imaging include amino acids[14,16,34,35], oligosaccharides[19], carbonhydrate[18], Proteins[20,], Peptides[24], Lipids[22,23] and other plant metabolites[15-17]. The technique has also been proven to be useful in the monitoring of metabolites of nitrogen fixing bacteria known as rhizobia[36]. MS imaging, of stable isotope labelled compounds will therefore clearly be a useful tool in the future for monitoring the distribution of other species with in plants, since this technique could to be used to monitor the uptake and distribution of herbicides, pesticides and plant growth regulator (PGR) not only within the primary plant they were applied but also in second generation plant. It could also be used to monitor bioremediation and show if plants have been grown on contaminated land. It also has the potential to help optimize plant nutrition, nutrient delivery and schedules.

## Conclusion

The data presented here have demonstrated that atoms and molecules move from dead plant material into new living material and that MALDI-MS and TOF-SIMS imaging are useful tools for monitoring the distribution of compounds with in plants and that the use of stable isotope labelled compounds in MS imaging experiments can yield useful information about uptake and fate in metabolomics based experiments.
Mass spectrometry imaging has been used to demonstrate the uptake of labeled nitrogen species from composted radish leaves into growing radish plants. The "cycle" of life has been successfully demonstrated.

## Acknowledgements

The authors would like to thank Gareth Hopcroft and Ian Stansfield from Aquaculture Ltd for helpful advice on hydroponic systems for plant growth.

## References

[1] BBC Four, AfterLife: The Strange Science of decay. http://www.bbc.co.uk/programmes/b012w66t *(Accessed Nov* 2013).

[2] Scott, P. *Physiology and Behaviour of Plants;* John Wiley & Sons Ltd: Chichester, UK, 2008.

[3] Keeney, D. R.; Hatfield, J. L. In *Chapter 1 - The Nitrogen Cycle, Historical Perspective, and Current and Potential Future Concerns;* Follett, R. F., Hatfield, J. L., Eds.; Nitrogen in the Environment: Sources, Problems and Management; Elsevier Science: Amsterdam, 2001; pp 3-16.

[4] Berglund, M.; Wieser, M. E. Isotopic compositions of the elements 2009 (IUPAC Technical Report). *Pure and Applied Chemistry* **2011**, *83*, 397-410.

[5] Dawson, T. E.; Mambelli, S.; Plamboeck, A. H.; Templer, P. H.; Tu, K. P. *Annu. Rev. Ecol. Syst.* **2002**, *33*, 507-559.

[6] Engelsberger, W. R.; Erban, A.; Kopka, J.; Schulze, W. X. *Plant Methods* **2006**, *2*, 14.

[7] Fiedler, R.; Proksch, G. *Plant Soil* **1972**, *36*, 371-&.

[8] Heltai, G.; Jozsa, T. *Microchem. J.* **1995**, *51*, 245-255.

[9] Knicker, H.; Lüdemann, H. *Org. Geochem.* **1995**, *23*, 329-341.

[10] Lechene, C. P.; Luyten, Y.; McMahon, G.; Distel, D. L. *Science* **2007**, *317*, 1563-1566.

[11] Grignon, N.; Halpern, S.; Jeusset, J.; Briancon, C.; Fragu, P. *Journal of Microscopy-Oxford* **1997**, *186*, 51-66.

[12] Marsh, K. L.; Sims, G. K.; Mulvaney, R. L. *Biol. Fertility Soils* **2005**, *42*, 137-145.

[13] Bichat, F.; Sims, G. K.; Mulvaney, R. L. *Soil Sci. Soc. Am. J.* **1999**, *63*, 100-110.

[14] Kaspar, S.; Peukert, M.; Svatos, A.; Matros, A.; Mock, H. *Proteomics* **2011**, *11*, 1840-1850.

[15] Lee, Y. J.; Perdian, D. C.; Song, Z.; Yeung, E. S.; Nikolau, B. J. *The Plant Journal* **2012**, *70*, 81-95.

[16] Burrell, M. M.; Earnshaw, C. J.; Clench, M. R.. *J. Exp. Bot.* **2007**, *58*, 757-763.

[17] Li, Y.; Shrestha, B.; Vertes, A. *Anal. Chem.* **2008**, *80*, 407-420.

[18] Robinson, S.; Warburton, K.; Seymour, M.; Clench, M.; Thomas-Oates, J.. *New Phytol.* **2007**, *173*, 438-444.

[19] Wang, J.; Sporns, P.; Low, N. H. *J. Agric. Food Chem.* **1999**, *47*, 1549-1557.

[20] Grassl, J.; Taylor, N. L.; Millar, A. H. *Plant Methods* **2011**, *7*, 21.

[21] Schwartz, S. A.; Reyzer, M. L.; Caprioli, R. M. *Journal of Mass Spectrometry* **2003**, *38*, 699-708.

[22] Vrkoslav, V.; Muck, A.; Cvacka, J.; Svatos, *J. Am. Soc. Mass Spectrom.* **2010**, *21*, 220-231.

[23] Horn, P. J.; Korte, A. R.; Neogi, P. B.; Love, E.; Fuchs, J.; Strupat, K.; Borisjuk, L.; Shulaev, V.; Lee, Y.; Chapman, K. D. *Plant Cell* **2012**, *24*, 622-636.

[24] Kondo, T.; Sawa, S.; Kinoshita, A.; Mizuno, S.; Kakimoto, T.; Fukuda, H.; Sakagami, Y. *Science* **2006**, *313*, 845-848.

[25] Anderson, D. M. G.; Carolan, V. A.; Crosland, S.; Sharples, K. R.; Clench, M. R. *Rapid Communications in Mass Spectrometry* **2009**, *23*, 1321-1327.

[26] Mullen, A. K.; Clench, M. R.; Crosland, S.; Sharples, K. R. *Rapid Communications in Mass Spectrometry* **2005**, *19*, 2507-2516.

[27] Trim, P. J.; Djidja, M.; Atkinson, S. J.; Oakes, K.; Cole, L. M.; Anderson, D. M. G.; Hart, P. J.; Francese, S.; Clench, M. R. *Analytical and Bioanalytical Chemistry*. **2010**, *397*, 3409-3419.

[28] Strohalm, M.; Kavan, D.; Novak, P.; Volny, M.; Havlicek, V. *Anal. Chem.* **2010**, *82*, 4648-4651.

[29] Wu, X. L.; Prior, R. L. *J. Agric. Food Chem.* **2005**, *53*, 3101-3113.

[30] Mihaylova, V.; Lyubomirova, V.; Djingova, R. *Int. J. Environ. Anal. Chem.* **2013**, *93*, 1441-1456.

[31] Lombi, E.; Scheckel, K. G.; Kempson, I. M. *Environ. Exp. Bot.* **2011**, *72*, 3-17.

[32] Wu, B.; Zoriy, M.; Chen, Y.; Becker, J. S. *Talanta* **2009**, *78*, 132-137.

[33] Wu, B.; Becker, J. S. *Metallomics* **2012**, *4*, 403-416.

[34] Gogichaeva, N. V.; Alterman, M. A. *Methods Mol. Biol.* **2012**, *828*, 121-35.

[35] Gogichaeva, N. V.; Williams, T.; Alterman, M. A. *J. Am. Soc. Mass Spectrom.* **2007**, *18*, 279-284.

[36] Ye, H.; Gemperline, E.; Venkateshwaran, M.; Chen, R.; Delaux, P.; Howes-Podoll, M.; Ane, J.; Li, L. *Plant J.* **2013**, *75*, 130-145.

**Figure legends**

**Figure 1**: Experimental workflow used in this study.

**Figure 2:** MALDI-MS images showing the distribution of unlabelled and $^{15}N$ labelled choline at m/z 104 and 105 repectively within (a) the bulbs and (b) the leaves of the control, first generation labelled $^{15}N$ radish and a second generation radish grown using a tea created from the first generation plants. (Normalized against the TIC).

**Figure 3:** MALDI-MS spectra obtained from the leaves of the a) control, b) $^{15}N$ radish and c) second generation $^{15}N$ plant.

**Figure 4:** MALDI-MSI images showing the distribution of A) a species identified as the anthrocyanidin pelargonadin at m/z 271, B) choline at m/z 104, C) $^{15}N$ labelled choline at m/z 105, D) phosphocholine at m/z 184, E) $^{15}N$ labelled phosphocholine at m/z 185, F) $^{15}N$ labelled choline at m/z 105 overlaid onto the unknown species at m/z 271 and G) $^{15}N$ labelled phosphocholine at m/z 185 overlaid onto pelargonadin species at m/z 271.

**Figure 5:** A) Optical image of the control radish section and TOF-SIMS images showing B) the total ion current, the distribution of C) choline at m/z 104 and D) C13 isotope of choline at m/z 105 and E) TOF-SIMS spectrum obtained from the radish tissue section.

**Figure 6:** A) Optical image of the first generation radish section and TOF-SIMS images showing B) the total ion current, the distribution of C) choline at m/z 104 and D) $^{15N}$ labeled choline at m/z 105 and E) TOF-SIMS spectrum obtained from the radish tissue section.

**Figure 7:** A) Optical image of the second generation radish section and TOF-SIMS images showing B) the total ion current, the distribution of C) $^{15}N$ labelled choline at m/z 105 and D) choline at m/z 104 and E) TOF-SIMS spectrum obtained from the radish tissue section.

**Figure S1**: MALDI-MS/MS spectrum showing the product ions derived from a) choline at m/z 104 and b)$^{15}N$ labelled choline at m/z 105.

**Figure S2:** MALDI-MS/MS spectrum showing the product ions, derived from the precursor ion of Pelargonidin at m/z 271.12.

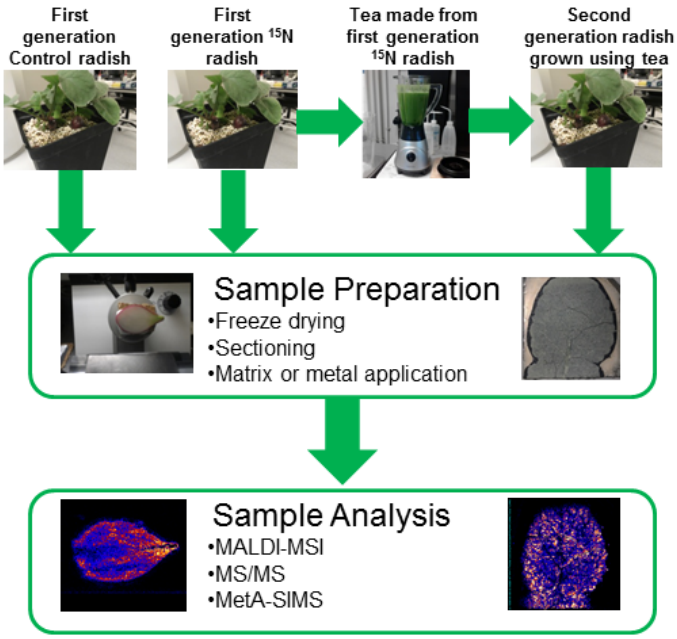
First generation Control radish
First generation $^{15}$N radish
Tea made from first generation $^{15}$N radish
Second generation radish grown using tea
Sample Preparation
•Freeze drying
•Sectioning
•Matrix or metal application
Sample Analysis
•MALDI-MSI
•MS/MS
•MetA-SIMS

359

360

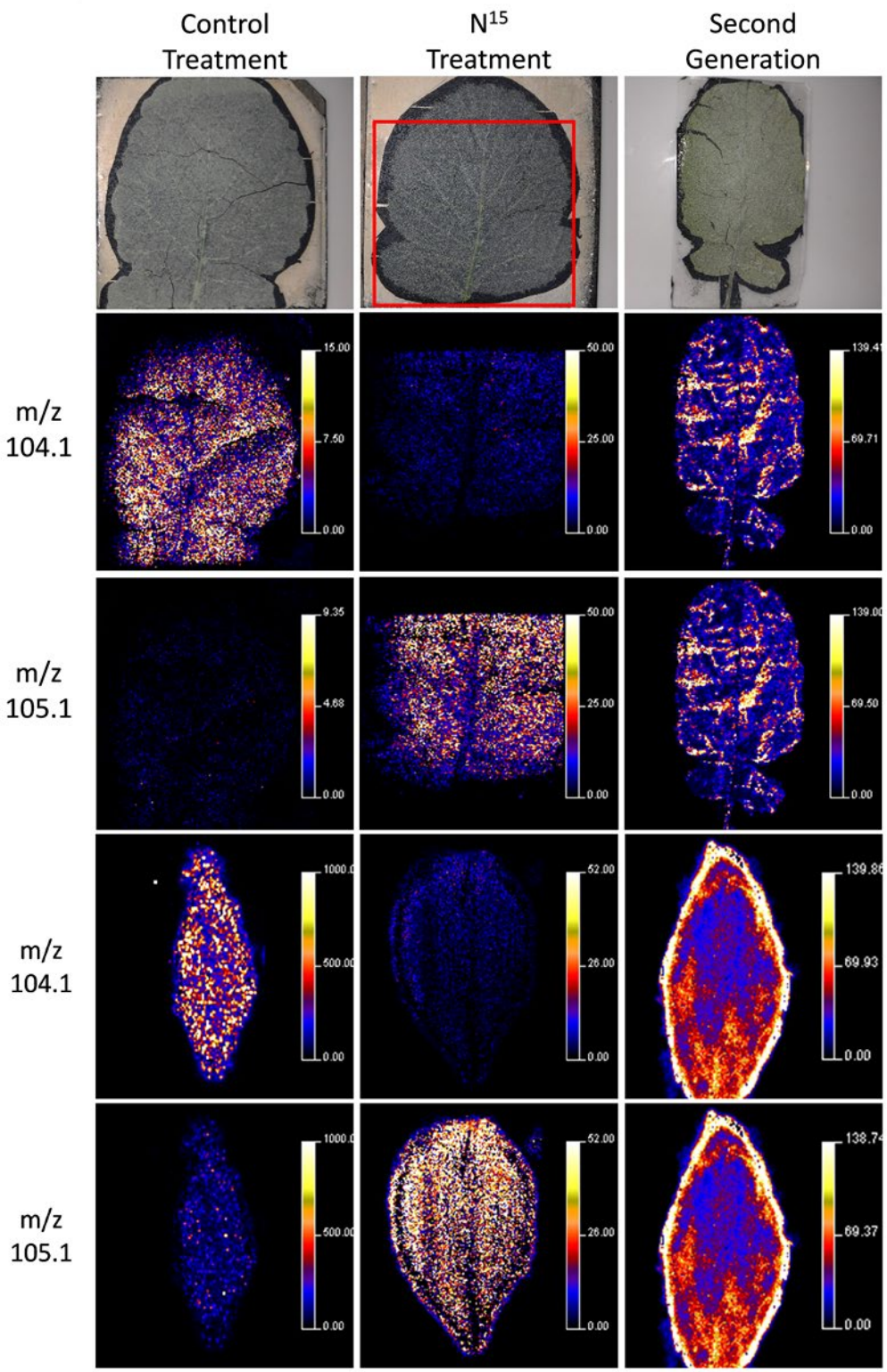
Control Treatment
N15 Treatment
Second Generation
m/z 104.1
m/z 105.1
m/z 104.1
m/z 105.1

361

362

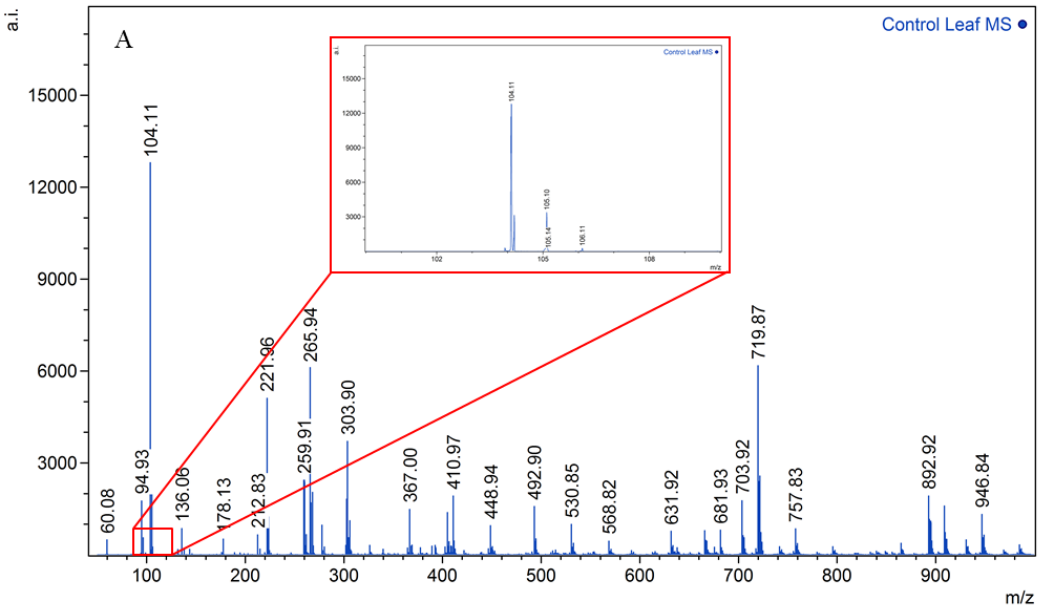
A
Control Leaf MS
a.i.
m/z
104.11
719.87
265.94
221.96
303.90
94.93
136.06
259.91
367.00
410.97
448.94
492.90
530.85
568.82
631.92
681.93
703.92
757.83
892.92
946.84
60.08
178.13
212.83

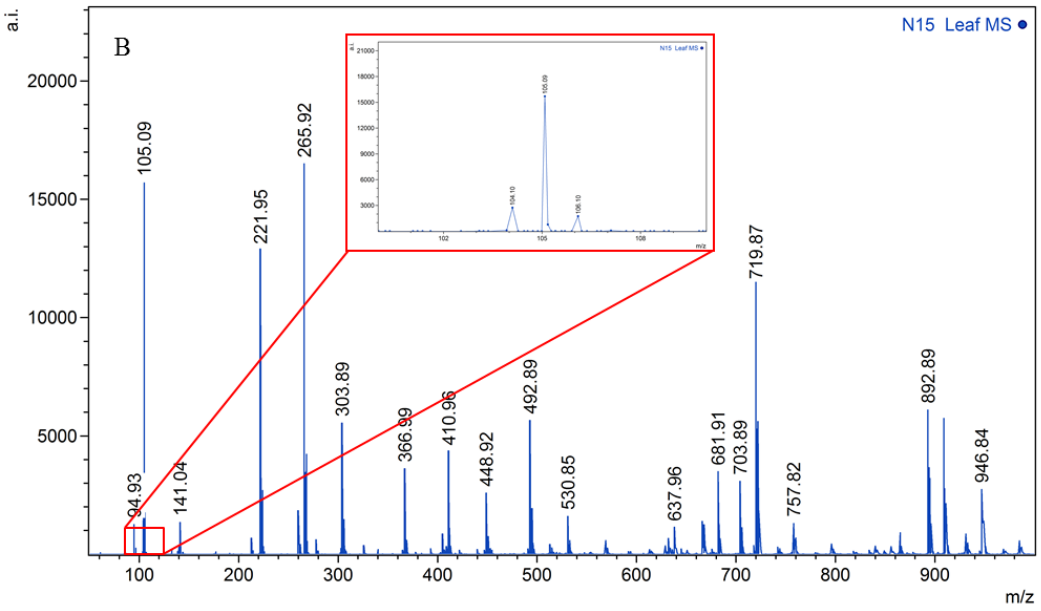
B
N15 Leaf MS
a.i.
m/z
105.09
265.92
221.95
719.87
303.89
366.99
410.96
492.89
892.89
946.84
94.93
141.04
448.92
530.85
637.96
681.91
703.89
757.82

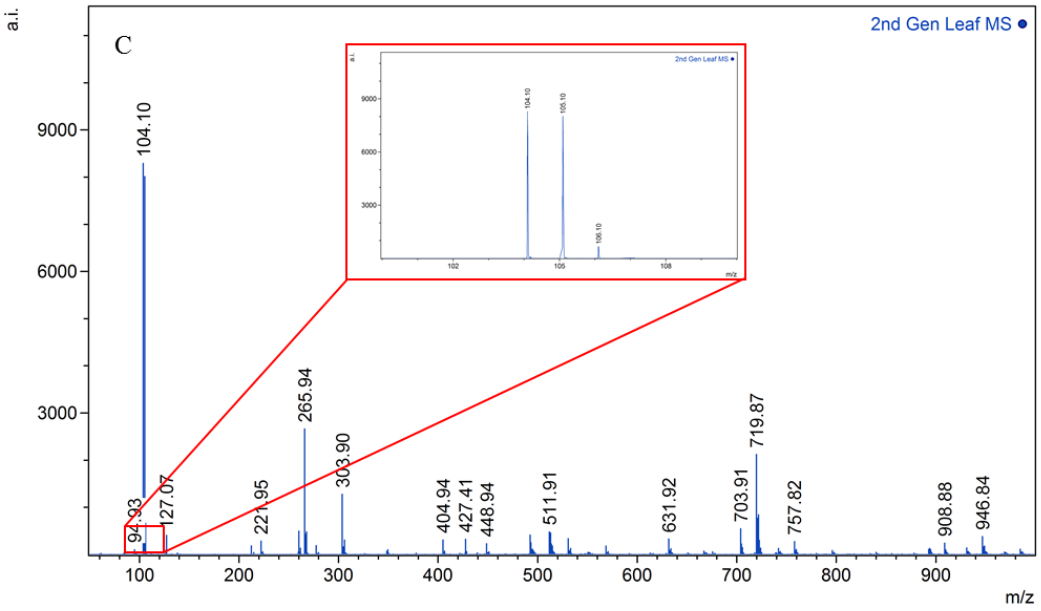
C
2nd Gen Leaf MS
a.i.
m/z
104.10
265.94
719.87
303.90
94.93
127.07
221.95
404.94
427.41
448.94
511.91
631.92
703.91
757.82
908.88
946.84

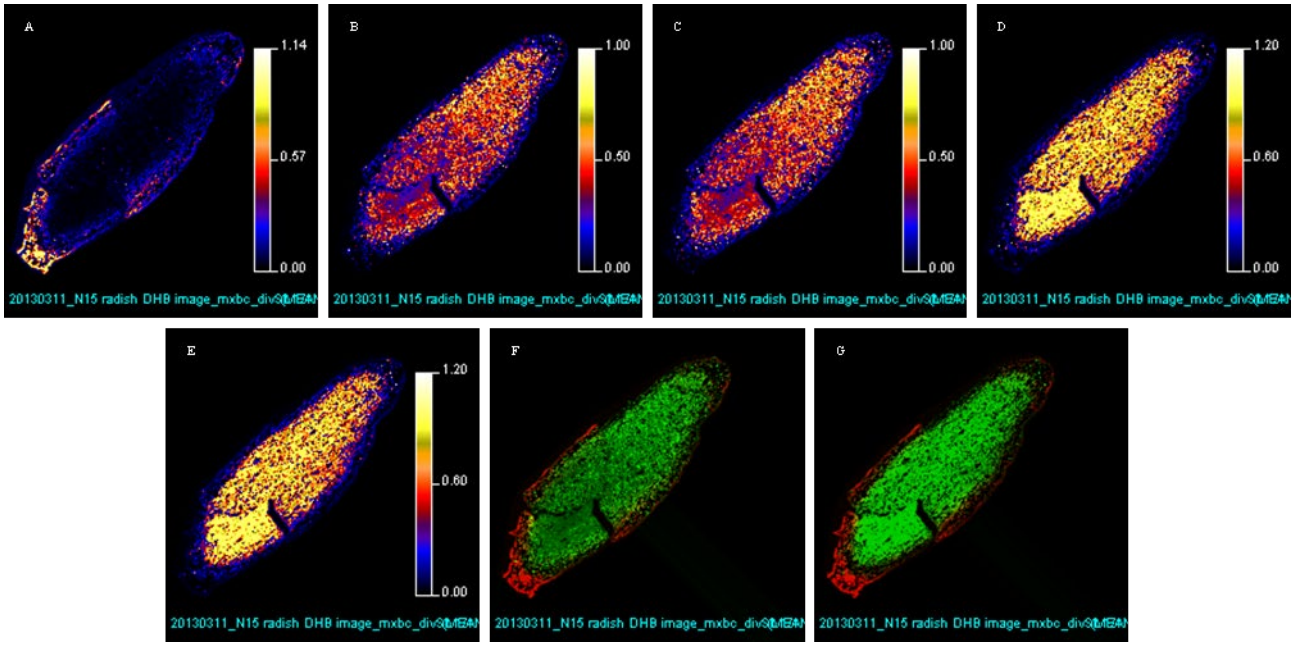
A
1.14
0.57
0.00
20130311_N15 radish DHB image_mxbc_div
B
1.00
0.50
0.00
20130311_N15 radish DHB image_mxbc_div
C
1.00
0.50
0.00
20130311_N15 radish DHB image_mxbc_div
D
1.20
0.60
0.00
20130311_N15 radish DHB image_mxbc_div
E
1.20
0.60
0.00
20130311_N15 radish DHB image_mxbc_div
F
20130311_N15 radish DHB image_mxbc_div
G
20130311_N15 radish DHB image_mxbc_div

364

365

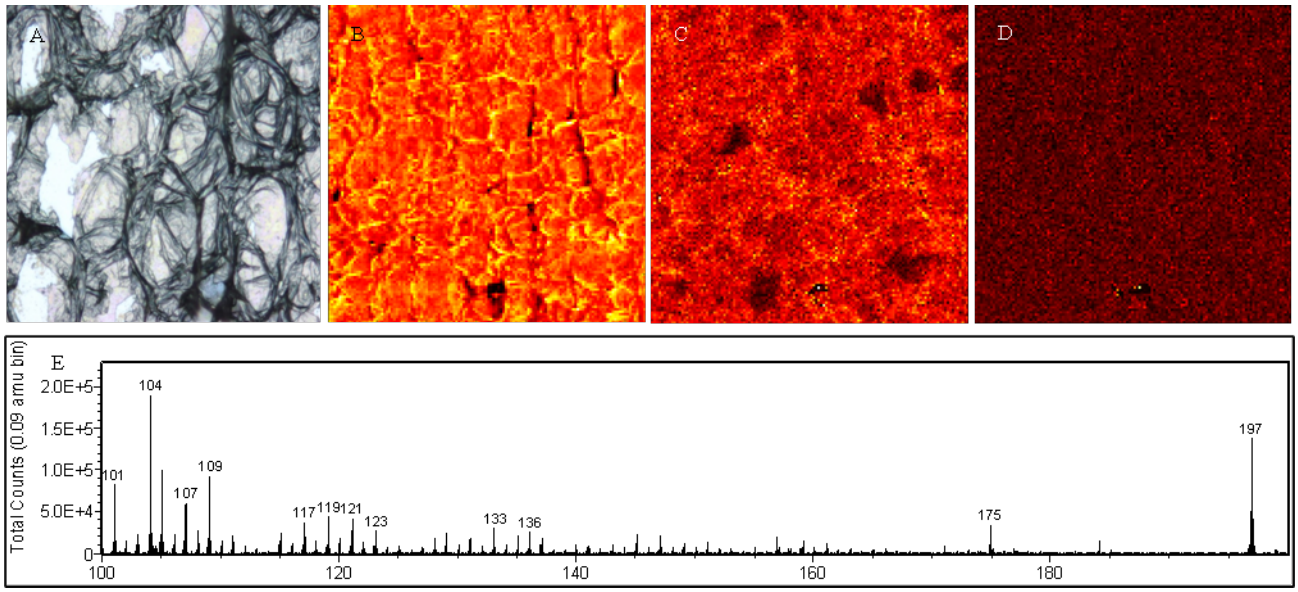
A
B
C
D
E
Total Counts (0.09 amu bin)
2.0E+5
1.5E+5
1.0E+5
5.0E+4
0
101
104
107
109
117
119
121
123
133
136
175
197
100
120
140
160
180

366

367

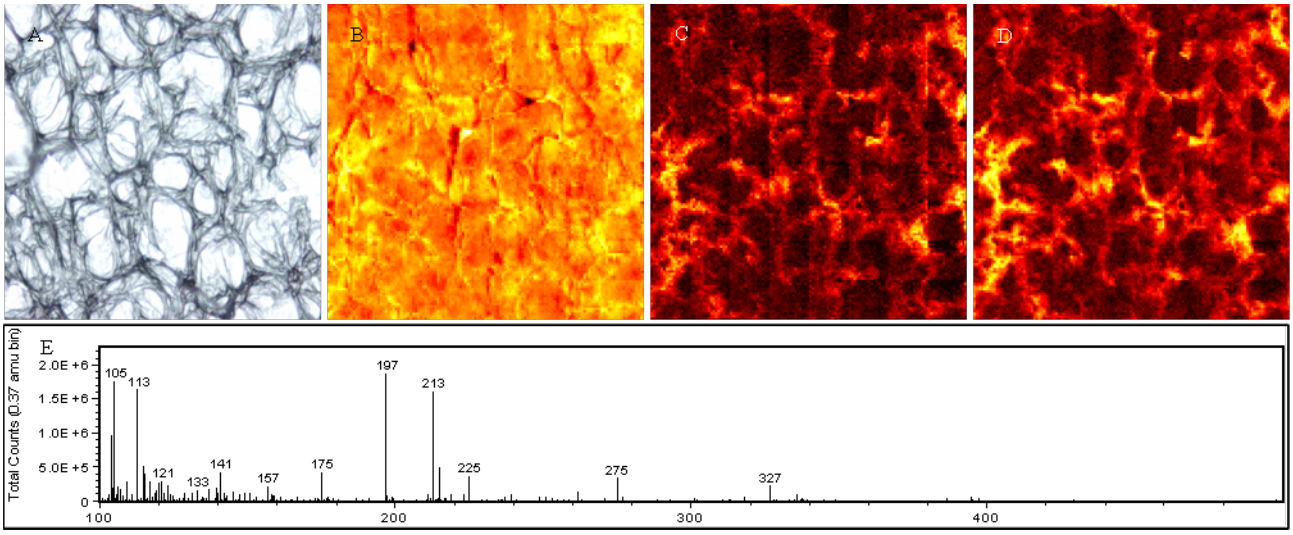
A
B
C
D
E
Total Counts (0.37 amu bin)
2.0E+6
1.5E+6
1.0E+6
5.0E+5
0
105
113
121
133
141
157
175
197
213
225
275
327
100
200
300
400

368

369

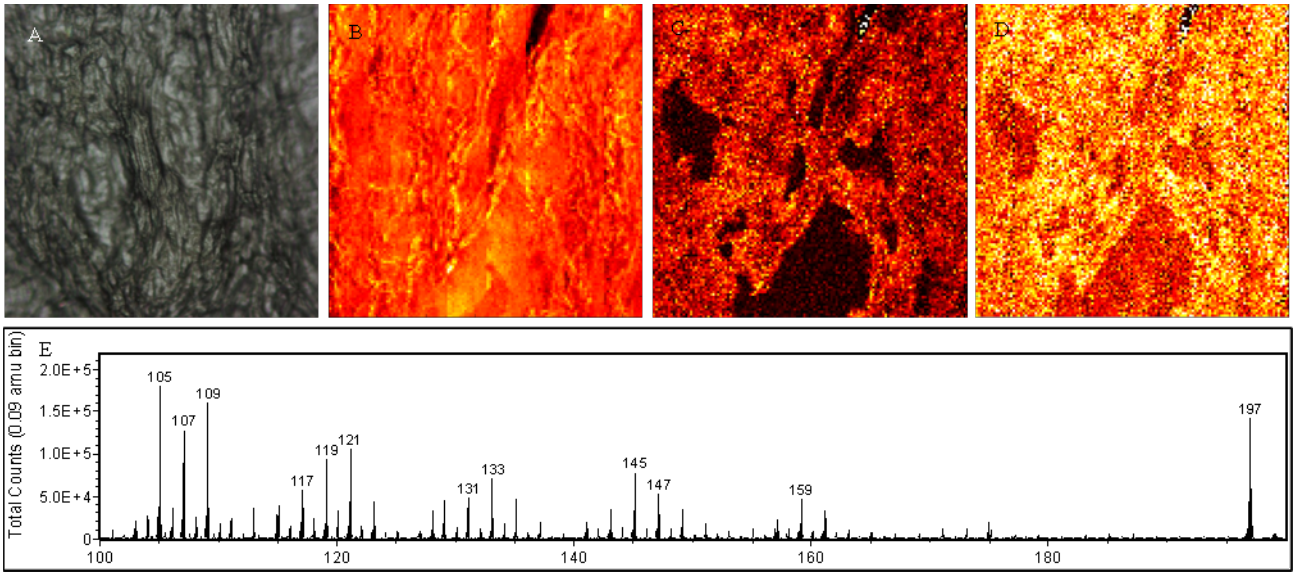
A
B
C
D
E
Total Counts (0.09 amu bin)
2.0E+5
1.5E+5
1.0E+5
5.0E+4
0
105
107
109
117
119
121
131
133
145
147
159
197
100
120
140
160
180

370

371

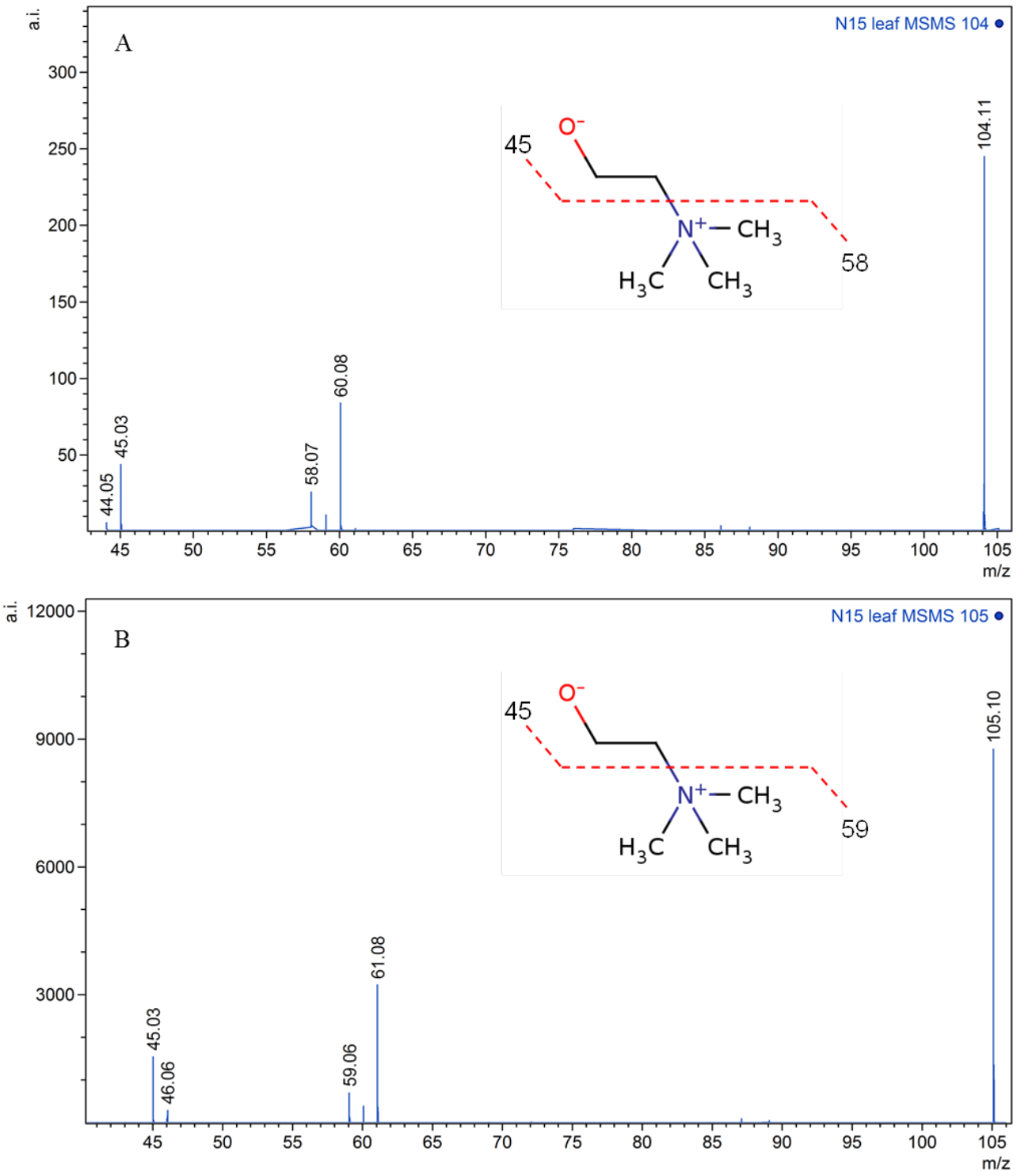
A
N15 leaf MSMS 104
a.i.
104.11
60.08
45.03
58.07
44.05
45
58
m/z
B
N15 leaf MSMS 105
105.10
61.08
45.03
46.06
59.06
59

372

373

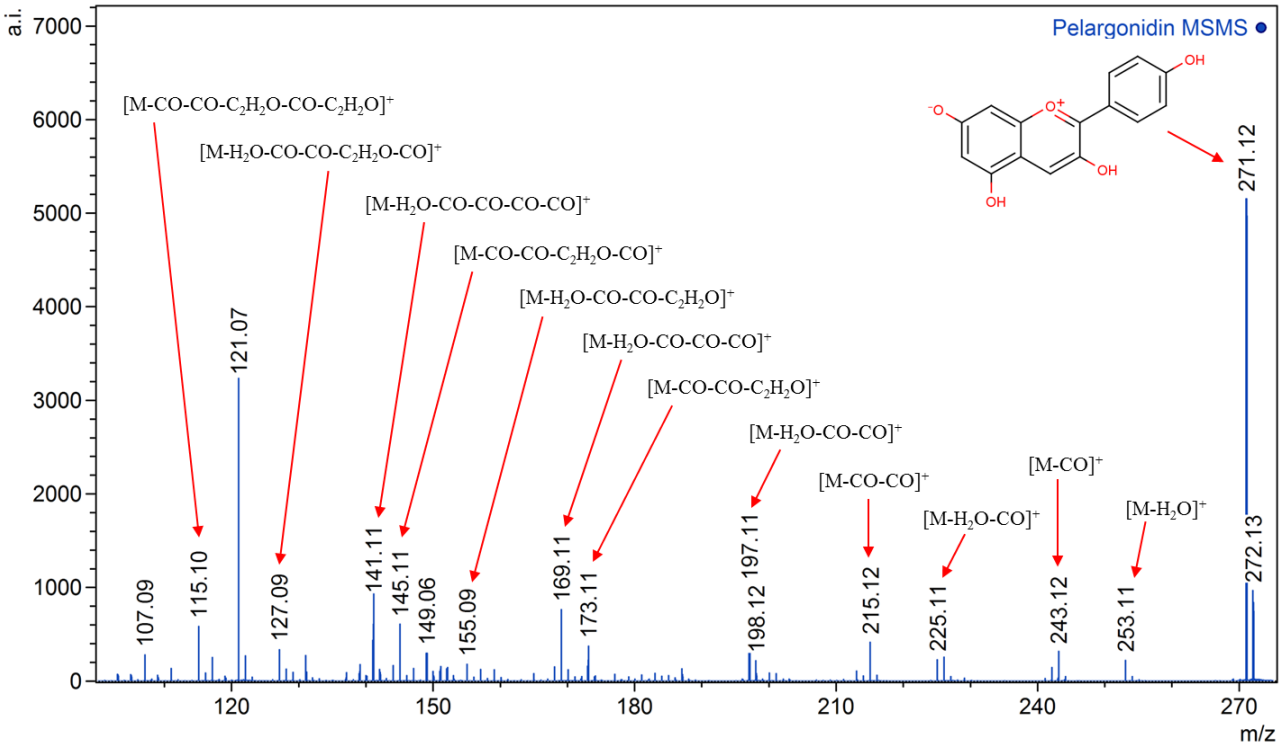
Pelargonidin MSMS
a.i.
m/z
[M-CO-CO-C2H2O-CO-C2H2O]+
[M-H2O-CO-CO-C2H2O-CO]+
[M-H2O-CO-CO-CO-CO]+
[M-CO-CO-C2H2O-CO]+
[M-H2O-CO-CO-C2H2O]+
[M-H2O-CO-CO-CO]+
[M-CO-CO-C2H2O]+
[M-H2O-CO-CO]+
[M-CO-CO]+
[M-H2O-CO]+
[M-CO]+
[M-H2O]+
107.09
115.10
121.07
127.09
141.11
145.11
149.06
155.09
169.11
173.11
197.11
198.12
215.12
225.11
243.12
253.11
271.12
272.13

374